Neutron and x-ray diffraction study and symmetry analysis of phase transformations in lower tungsten carbide W_2C

A. S. Kurlov and A. I. Gusev
Institute of Solid State Chemistry, Ural Division of the Russian Academy of Sciences, Pervomaiskaya 91, GSP-145, Ekaterinburg 620041, Russia
(Received 15 August 2007; published 28 November 2007)

The literature data on the crystal structure of disordered and different ordered phases of the lower tungsten carbide W_2C are contradictory. In this context, the symmetry analysis of all possible superstructures of the carbide W_2C is performed and the physically possible sequence of phase transformations in W_2C carbide is established. Atomic and vacancy ordering in the lower tungsten carbide W_2C with the basic hexagonal structure of the $L'3$ type is studied by the neutron and x-ray diffraction methods. It is found that the trigonal ε-W_2C phase (space group $P\bar{3}1m$) is the only ordered phase of the lower tungsten carbide over a wide temperature interval of ~2300–1370 K. Trigonal phase ε-W_2C is formed at a temperature of ~1900–2300 K most likely by the mechanism of the second-order phase transition. The disorder-order phase transition channel and the structure of the trigonal carbide ε-W_2C are determined. The carbon atom distribution function is calculated for the trigonal ε-W_2C superstructure. The distribution of carbon atoms in the trigonal ε-W_2C phase is described by two long-range order parameters η_{15} and η_{17}. It is shown that the lower tungsten carbide does not undergo solid-phase decomposition to W and WC over the investigated temperature interval from 2300 to 1370 K. The phase diagram of the W-C system is refined considering data obtained for the ε-W_2C phase.

DOI: 10.1103/PhysRevB.76.174115 PACS number(s): 61.50.Ks, 61.66.Fn, 64.70.Kb, 81.30.Dz

I. INTRODUCTION

Atomic ordering of strongly nonstoichiometric compounds such as carbides, nitrides, and oxides of transition metals is a very widespread but poorly understood phenomenon. The study of atomic ordering in relation to nonstoichiometry is part of such general problem of solid state physics as disorder-order phase transformations in defect solids.

Carbides MC_y and M_2C_y of transition d metals of groups IV-VI belong to the class of strongly nonstoichiometric interstitial compounds.[1,2] They are known as the most high-melting and hardest compounds.[1–3]

Carbon atoms fill octahedral interstices of the metal sublattice in carbides and form nonmetal sublattice. Unfilled (vacant) interstices are called structural vacancies □. Structural vacancies and carbon atoms form a substitutional solution in the nonmetal sublattice. The distribution of C atoms and vacancies □ over lattice sites can be disordered (statistical) or ordered.

While ordering in higher cubic carbides MC_y has been well studied,[1,2,4–6] ordering in lower carbides M_2C_y $(0.7<y\leqslant 1.0)$, which have a hexagonal structure, is by far less known. The lower tungsten carbide W_2C_y is the least understood compound among lower carbides.

The lower tungsten carbide W_2C_y belongs to strongly nonstoichiometric interstitial compounds[1,2] and its homogeneity interval is $WC_{0.34}$ to $WC_{0.52}$ at a temperature of ~3000 K.[7] As the temperature decreases, the homogeneity interval shrinks. Four modifications of the lower tungsten carbide W_2C_y are described to a certain extent or mentioned in the literature. Tungsten atoms form a hexagonal closely packed metal sublattice in all the modifications of the carbide W_2C_y. In this sublattice, 34%–36% to 50%–52% octahedral interstices can be occupied by carbon atoms, while the other interstices are vacant. Depending on the distribution of C atoms and structural vacancies □, the lower carbide W_2C_y can be disordered at a high temperature or ordered at a low temperature. The sequence of phase transformations in the lower tungsten carbide W_2C_y is still unknown. The theoretical symmetry analysis of ordering in the lower tungsten carbide β-W_2C (W_2C) has never been performed before.

The prime objective of this study is experimental and theoretical analysis of atomic and vacancy ordering in the carbon sublattice of the lower tungsten carbide W_2C. Therefore, we shall consider available data on the crystal structure of this carbide in more detail.

II. CRYSTAL STRUCTURE OF PHASES OF THE LOWER TUNGSTEN CARBIDE W_2C (REVIEW)

The high-temperature basic phase β-W_2C has a hexagonal [space group $P6_3/mmc$ (D^4_{6h})] structure of the $L'3$ type (Fig. 1) with a disordered arrangement of C atoms and structural vacancies □ in the nonmetal sublattice. This phase is stable over the temperature interval starting from 2300 to 2400 or 2670 to 2720 K and ending with the melting temperature of 3000–3050 K. Direct experimental evidence to the existence of the lower tungsten carbide with the $L'3$-type structure is adduced by a neutron diffraction study,[8] in which the disordered carbide β-W_2C was observed simultaneously with an ordered phase of this carbide.

Three ordered phases of the carbide W_2C are mentioned in the literature: orthorhombic β'-W_2C [Space Group No. 60, $Pbcn$ (D^{14}_{2h})] with the ζ-Fe_2N (Mo_2C) structure, rhombohedral β''-W_2C [Space Group No. 164, $P\bar{3}m1$ (D^3_{3d})] with the $C6$ (anti-CdI_2) structure, and trigonal ε-W_2C [Space Group No. 162, $P\bar{3}1m$ (D^1_{3d})] with the ε-Fe_2N structure. In some studies, the orthorhombic carbide β'-W_2C is labeled ζ-W_2C and the rhombohedral carbide β''-W_2C is labeled α-W_2C.

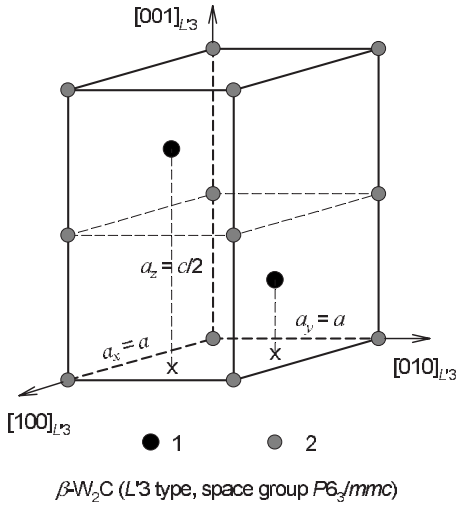

FIG. 1. Unit cell of the basic disordered hexagonal (space group $P6_3/mmc$) phase β-W_2C of the lower tungsten carbide with the structure of the $L'3$ type (lattice constants of the unit cell are equal to a in the directions $[100]_{L'3}$ and $[010]_{L'3}$ and c in the direction $[001]_{L'3}$). The primitive (concerning the nonmetal sublattice) cell is shown with a dashed line. Lattice constants a_x and a_y of the primitive cell coincide with the corresponding lattice constants of the unit cell; the lattice constant a_z of the primitive cell in the direction $[001]_{L'3}$ is twice as small as the lattice constant c of the unit cell, i.e., $a_z=c/2$. (1) W atoms and (2) nonmetal sublattice sites statistically (with the probability of 1/2) occupied by C atoms.

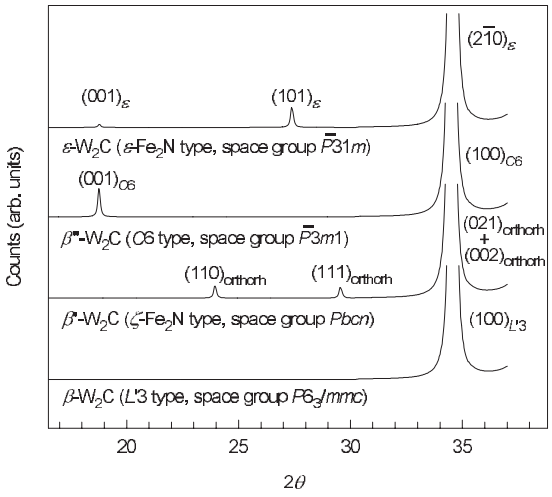

FIG. 2. Calculated XRD patterns of modifications β-W_2C, β'-W_2C, β''-W_2C, and ε-W_2C of the lower tungsten carbide W_2C differ only over the interval of small angles 2θ. Intensities of the reflections $(110)_{\text{orthorh}}$ and $(111)_{\text{orthorh}}$ characteristic of the orthorhombic carbide β'-W_2C, the reflection $(110)_{C6}$ characteristic of the rhombohedral carbide β''-W_2C, and the reflection $(101)_\varepsilon$ characteristic of the trigonal carbide ε-W_2C account for less than 0.5% of the intensity of the strongest reflection $(101)_{L'3}$ [or $(110)_{C6}$, $(002)_{\text{orthorh}}$, and $(2-10)_\varepsilon$ of the corresponding structure]. Calculations are made for perfect (disregarding atomic displacements) structures of the lower carbide W_2C with composition $WC_{0.50}$. Cu $K\alpha_{1,2}$ radiation.

Some researchers determined the structure of the ordered phases of the lower tungsten carbide by the x-ray diffraction method using powdered samples, while others used the neutron diffraction study. In this connection, before we proceed to the discussion of the literature data, let us dwell briefly on capabilities of these methods as applied to the tungsten carbide W_2C.

The modifications β-W_2C, β'-W_2C (ζ-W_2C), β''-W_2C, and ε-W_2C of the lower tungsten carbide W_2C are practically indiscriminate in powder x-ray diffraction experiments. This is because they have similar hexagonal metal sublattices, while the x-ray scattering amplitudes of W atoms is many times larger than that of C atoms. According to calculations, the change of the distribution of carbon atoms in the W_2C lattice influences x-ray diffraction spectra at small angles only (Fig. 2). Intensities of the reflections $(110)_{\text{orthorh}}$ and $(111)_{\text{orthorh}}$, which are characteristic of the orthorhombic carbide β'-W_2C, the reflection $(001)_{C6}$ of the carbide β''-W_2C with the $C6$ structure, and the reflection $(101)_\varepsilon$ typical of the carbide ε-W_2C account for less than 0.5% of the intensity of the strongest reflection $(101)_{L'3}$ [or reflections $(100)_{C6}$, $(002)_{\text{orthorh}}$, and $(2-10)_\varepsilon$ of the corresponding structures]. Thus, these reflections are at the background level and are less than the experimental intensity error in x-ray diffraction studies. In this connection, results of some investigations, in which the structure of the ordered phases of the lower tungsten carbide was determined only by the powder x-ray diffraction method, are not quite reliable. However, the presence of atomic displacements in the ordered phases can lead to specific splitting of some diffraction reflections. Then, the symmetry of a particular phase can be assessed qualitatively.

A more informative method for the analysis of ordering in the nonstoichiometric tungsten carbide is neutron diffraction because the intensities of neutron scattering by tungsten and carbon nuclei are comparable. In neutron diffraction experiments, the redistribution of carbon atoms in the carbide W_2C is followed by a considerable change of the intensity of diffraction reflections and appearance of measurable superstructure reflections specific of each ordered phase. Preliminary calculations of neutron diffraction patterns of the disordered hexagonal lower carbide β-W_2C ($WC_{0.50}$) and perfect ordered phases β'-W_2C (ζ-W_2C), β''-W_2C, and ε-W_2C having the orthorhombic, the rhombohedral, and the trigonal symmetry demonstrated that superstructure reflections characteristic of these phases can be observed over the interval of small angles $2\theta<33°$ (Fig. 3).

Taking into account the aforementioned capabilities of the x-ray and neutron diffraction methods, let us consider literature data on ordering in the lower tungsten carbide.

Rudy and co-workers[9–11] claimed the existence of the orthorhombic phase β'-W_2C when they analyzed the x-ray powder pattern of a W_2C sample quenched from 2630 K and reviewed differential thermal analysis data. According to Ref. 9, the phase β'-W_2C is stable at temperatures of ~2370–2750 K. The structure of the orthorhombic (space group $Pbcn$) phase β'-W_2C was proposed[9] by analogy with the ordered molybdenum carbide Mo_2C.[12] The same assumption on the crystal structure of the orthorhombic phase β'-W_2C was done by Stecher *et al.*[13] who studied phase

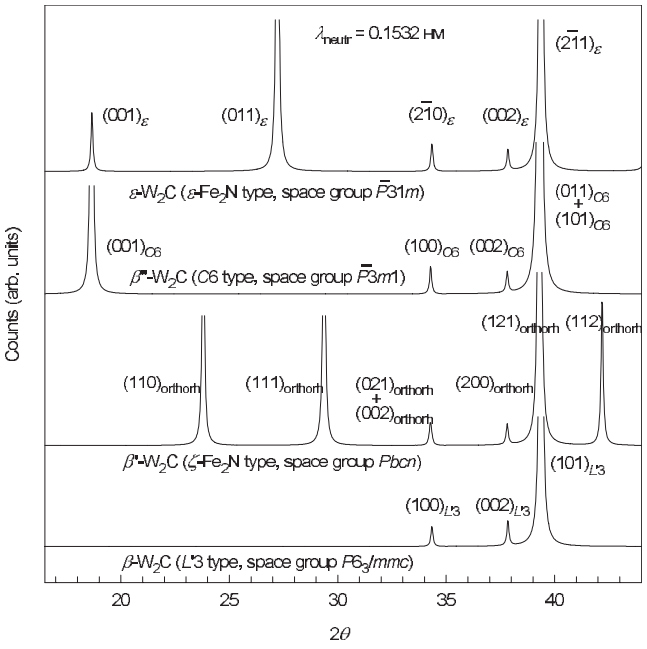

FIG. 3. Calculated neutron diffraction patterns ($\lambda=0.1532$ nm) of the disordered hexagonal ($L'3$ type, space group $P6_3/mmc$) carbide β-W_2C ($WC_{0.50}$) and perfect ordered phases β'-W_2C (ζ-W_2C), β''-W_2C, and ε-W_2C with the orthorhombic (ζ-Fe_2N type, space group $Pbcn$), rhombohedral ($C6$ type, space group $P\bar{3}m1$), and trigonal (ε-Fe_2N type, space group $P\bar{3}1m$) symmetries.

equilibria in the Cr-W-C system. However, in powder x-ray experiments, the change of the carbon atom distribution in the nonmetal sublattice of the lower tungsten carbide has little effect on the x-ray diffraction spectrum at $2\theta<30°$ only (Fig. 2), whereas in Ref. 9 the first reflection was observed at $2\theta=34.55°$. Thus, the study[9] did not provide any experimental structural data confirming the existence of the orthorhombic tungsten carbide β'-W_2C at temperatures of 2370–2750 K.

Telegus *et al.*[14,15] prepared W_2C ($WC_{0.50}$) samples by hot pressing of a mixture of tungsten and carbon powders and its subsequent smelting in an electric-arc furnace. Then, the W_2C ($WC_{0.50}$) samples were annealed in a vacuum at 1470, 1370, 1270, 1170, and 1070 K for 600 h. Some diffraction reflections of the basic hexagonal lattice were split in x-ray patterns of samples annealed at $T\leqslant 1270$ K. Calculations[14] showed that the observed XRD pattern corresponds to the ordered orthorhombic phase β'-W_2C having the structure of the ζ-Fe_2N type. The ordered orthorhombic (space group $Pbcn$) phase β'-W_2C was still present in W_2C samples[15] annealed at 870, 1070, and 1270 K for 3000, 1500, and 750 h, respectively. Samples of W_2C ($WC_{0.50}$), which were annealed at 1070–1270 K for 600 h, were studied[16] in addition by the neutron diffraction method. The analysis revealed the presence of the ordered orthorhombic (space group $Pbcn$) phase β'-W_2C, in which ~85% carbon atoms were ordered. However, the Nozik *et al.*[16] gave incorrect coordinates (1/4 1/4 1/2) of positions 8(d) occupied by atoms W in the β'-W_2C structure. Atoms in the orthorhombic unit cell have the following coordinates: W atoms occupy positions 8(d) with the coordinates (1/4 ~ 1/8 ~ 1/12), while C atoms are in positions 4(c) with the coordinates (0 ~ 3/8 1/4). Morton *et al.*[17] detected the orthorhombic phase β'-W_2C in samples obtained by carburization of tungsten wires in xylene at ~2300–2800 K and subsequent annealing of wires carburized in a vacuum at 1170 K for 250 h. Later,[18] the orthorhombic phase β'-W_2C was observed by the x-ray method. Samples of W_2C were prepared by arc melting of W and WC mixtures with subsequent annealing at 2970 K for 1 h, decreasing of the temperature to 1120 K during 418 h, and final annealing at 1120 K for 146 h. Single crystals of W_2C having the size of 0.2–0.4 mm were taken from the annealed W_2C samples. These single crystals were used[18] for the x-ray determination of the ordered phase symmetry.

According to neutron diffraction data,[19,20] the orthorhombic phase β'-W_2C with the ζ-Fe_2N structure was observed in W_2C samples only after annealing at $T<1300$ K. Considering the results,[14–20] the orthorhombic (space group $Pbcn$) modification β'-W_2C (ζ-W_2C) exists at temperatures below 1300 K.

Rudy and Windisch[9] and Rudy and Hoffman[10] supposed the presence of the ordered rhombohedral phase β''-W_2C (α-W_2C) without adducing any structural evidence, while making reference to the paper.[21] This paper is dedicated to the electron diffraction analysis of the lower carbide W_2C prepared by carburization of a thin film of metallic tungsten in the carbon oxide CO at ~1400 K for 5 min. With limited data and without looking at other models, Butorina and Pinsker[21] conjectured that the lower carbide β''-W_2C has a rhombohedral [Space group No. 164, $P\bar{3}m1$ (D_{3d}^3)] structure of the $C6$ type (anti-CdI_2). According to Ref. 9, the phase β''-W_2C exists at temperatures of 2300–1500 K. Without adducing any structural evidence, Morton *et al.*[17] reported observation of the phase β''-W_2C (α-W_2C) in samples of the lower tungsten carbide prepared at temperatures of 2420–2520 K. The existence of the rhombohedral phase β''-W_2C was not confirmed afterward.

The trigonal (space group $P\bar{3}1m$) phase ε-W_2C was detected in W_2C samples synthesized by solid-phase sintering of tungsten and carbon mixtures at temperatures of 2370–2670 K,[8] 1920 K,[22] and 2070 K (Ref. 23) and those produced by arc melting[24] of tungsten and carbon mixtures. In Refs. 19, 20, and 25, the samples of the lower tungsten carbide were produced by annealing of carbon-saturated tungsten plates at 2370–2470 K. Then, the synthesized W_2C samples were ground and the powders were annealed at 1470 K for 100 h. Neutron diffraction patterns of the annealed powders of the lower tungsten carbide were taken at room temperature of 300 K and over the temperature interval of 1520–2070 K. The neutron and the electron diffraction analysis revealed[24] the trigonal carbide ε-W_2C with the structure of the ε-Fe_2N type in the annealed samples. Detailed neutron diffraction measurements[20] showed that the ordered trigonal (space group $P\bar{3}1m$) carbide ε-W_2C is the main phase and the hexagonal tungsten monocarbide WC is the impurity phase in the annealed powders. According to Ref. 20, the β-$W_2C \leftrightarrow \varepsilon$-$W_2C$ disorder-order transformation is the second-order transition, while the transition temperature changes between 1920 and 2100 K depending on the

TABLE I. Dependence of the lattice constants of a unit cell on the composition of trigonal carbide ε-W_2C (WC_y).

ε-W_2C (WC_y) carbide composition obtained from		Lattice constants of a unit cell (nm)		
Chemical analysis	Occupancies of nonmetal atomic positions of a unit cell	a	c	References
$WC_{0.415}$		0.5182	0.4720	19 and 20
$WC_{0.43}$		0.51833	0.47240	22
$WC_{0.445}$	$WC_{0.423}$	0.51852	0.47232	22
$WC_{0.45}$	$WC_{0.42}$	0.51809	0.47216	22
$WC_{<0.5}$		0.5184	0.4721	8
$WC_{0.460}$	$\sim WC_{0.50}$	0.5190	0.4724	19 and 20
$WC_{0.468}$		0.5194	0.4721	19 and 20

concentration of carbon in the lower tungsten carbide. As to the ordered orthorhombic (space group *Pbcn*) carbide β'-W_2C, it follows from neutron diffraction patterns[20] that a small amount of this carbide is formed in W_2C samples annealed at 1190–1300 K or lower. Annealing of the W_2C powder at 1170 K for 550 h led to the formation of the stable orthorhombic phase β'-W_2C.

The dependence of the unit cell lattice constants on the composition of the trigonal (space group $P\bar{3}1m$) carbide ε-W_2C (Refs. 8, 19, 20, 22, and 24) is given in Table I.

Samples of W_2C prepared by arc melting of W and WC mixtures with subsequent annealing at 1720–2120 K for 1.5 h and quenching to room temperature were studied[26,27] by the x-ray method. The structure was determined in W_2C single crystals 0.2–0.5 mm in size taken from quenched samples. Velikanava and co-workers[26,27] found that at a temperature of ~2120 K, the disordered lower carbide β-W_2C transforms to the trigonal ordered phase ε-W_2C. According to Ref. 27, the trigonal phase ε-W_2C is thermodynamically stable at temperatures of 2120–1520 K.

In addition to the assumption of the sequential phase transformations "disordered hexagonal phase β-W_2C $\rightarrow$ ordered orthorhombic phase β'-W_2C $\rightarrow$ ordered rhombohedral phase β''-W_2C," which take place in the lower tungsten carbide with decreasing temperature, it was conjectured[9,10] that at $T \leqslant 1530$ K, the carbide β''-W_2C decomposes to tungsten W and the higher carbide WC. To confirm their conjecture, Rudy and Windisch[9] and Rudy and Hoffman[10] referred to Ref. 28, in which the lower carbide W_2C could not be synthesized by sintering of a W and C mixture at a temperature of 1320 K for ~100 h.

The possible solid-phase decomposition of the lower tungsten carbide is also suggested by results reported in Ref. 27: two-phase (W+W_2C) and (W_2C+WC) samples, which were prepared by arc melting, were annealed at 1170 K for 850 h. The higher carbide WC was formed after low-temperature annealing of (W+W_2C) samples and tungsten W appeared after annealing of (W_2C+WC) samples. Therefore, Kublii and Velikanova[27] assumed that at a temperature of about 1520 K, the ordered trigonal phase ε-W_2C decomposes by an eutectoid reaction to tungsten W and the higher tungsten carbide WC, with the intermediate decomposition product being the metastable ordered orthorhombic (space group *Pbcn*) phase β'-W_2C having the ζ-Fe_2N structure. The same authors supposed the solid-phase decomposition of W_2C in their earlier study.[18] Notice that the assumption[18,27] of the eutectoid decomposition of the lower tungsten carbide contradicts results of the neutron diffraction:[20] there was no evidence that W_2C decomposed to W and WC when a single-phase sample of W_2C ($WC_{0.50}$) was annealed at 1170 K for a long time.

Although new experimental data on phase transformations in the lower tungsten carbide W_2C have appeared in the literature, handbooks on phase diagrams give 40 year old results for the W-C system that are not quite reliable. For example, the handbook[29] contains a generalized phase diagram of the W-C system, which was constructed using earlier phase diagrams[9–11] of this system and considering in part results of Ref. 30. The phase diagram of the W-C system in the handbook[31] is adopted from Refs. 10 and 11.

Thus, the literature data on ordering of the lower tungsten carbide W_2C and the temperature range of W_2C stability are contradictory and ambiguous. In this connection, the theoretical symmetry analysis of possible ordered phases of W_2C carbide is performed in this study. The crystal structure of the lower tungsten carbide, which was synthesized in different conditions over a wide temperature interval of ~3600–1370 K, is examined by the neutron and x-ray diffraction methods. An updated phase diagram of the W-C system is discussed considering experimental and theoretical results.

III. SAMPLES AND EXPERIMENT

Samples of the lower tungsten carbide W_2C were prepared by solid-phase sintering of W+C pressed powder mixtures in a vacuum of 0.0013 Pa (10^{-5} mm Hg) under three different temperature routes: (I) sintering at a temperature of 2070 K for 10 h; (II) annealing of the samples, which were sintered from tungsten and carbon at 2070 K, in a vacuum at T=1370 K for 35 h; (III) sintering of W+C powder mixtures in a vacuum at 1370 K for 50 h. A tungsten powder with particles of 3–5 μm in size and purity of 99.95% and carbon black with purity of 99.999% were the starting materials for

solid-phase vacuum sintering. The cylindrical samples 15 mm in diameter and 15–20 mm in length were fabricated by cold pressing of W+C powder mixtures at a pressure of 0.7 GPa without binders and then were placed in a graphite crucible for sintering. The W_2C powder was also produced by plasma chemical synthesis from the oxide WO_3 and propane C_3H_8 in hydrogen plasma at a temperature of ~3800 K. The reaction products condensed and were quenched near the reactor walls from a temperature of 2300–2400 K. The composition of the tungsten carbide samples obtained was certified by chemical and spectral methods. Chemical analysis of tungsten carbide samples obtained for carbon was carried out by Dumas gas chromatography on a Carlo Erba CHN 1108 analyzer. The oxygen contents of the starting powders and of the carbide samples were measured by a vacuum hot extraction equipment Balzers exhalograph EAO-201. The metal impurity contents of the starting powders and of the sintered samples were determined by inductively coupled plasma-mass spectrometry on a Spectromass 2000. The total impurity content of the samples as determined from the results of chemical and spectral analysis did not exceed 0.25 wt %.

The phase composition of the samples and the lattice constants of the phases were determined by the x-ray diffraction method in a DRON-UM1 diffractometer using Cu $K\alpha_{1,2}$ radiation at the angles 2θ between 10° and 140° in steps $\Delta 2\theta = 0.03°$ with the scan time of 2 s at each point.

The structure of the ordered phases of the lower carbide W_2C was studied by the neutron diffraction method using $D7a$ ($\lambda = 0.1532$ nm) and $D2$ ($\lambda = 0.1805$ nm) diffractometers installed in the horizontal channel of the research water-water atomic reactor IVV-2M (Zarechny, Russia). The diffractometer resolution $\Delta d/d$ was equal to 0.3%. The primary beam was monochromated by reflection of neutrons from two monochromators: neutrons were reflected in sequence from the (002) face of pyrolytic graphite and the (333) face of a Ge single crystal in the case of the $D7a$ diffractometer; in the case of the $D2$ diffractometer, neutron beam was reflected from the (111) face of a germanium single crystal and the (002) face of pyrolytic graphite. Neutron diffraction patterns were recorded at room temperature in a step-scanning mode with steps of $\Delta(2\theta) = 0.1°$ within the region 2θ from 5°–10° to 115°–125°. The neutron diffraction analysis of the plasma chemical W_2C powder was performed using the exposure times of 260 and 70 s at each point with neutrons having the wavelengths of 0.1532 and 0.1805 nm, respectively. Powder samples were kept in vanadium containers. Neutron diffraction measurements in compact sintered samples of W_2C were made with neutrons of wavelength of 0.1532 nm at the exposure time of 150 s per point. Sintered bulk samples of W_2C were fixed and were installed on a vertical aluminum holder. The GSAS program package[32] was used for phase structure refinements from powder data. Background was fitted by the Chebyshev sixth order polynomial. The reflection shape was modeled as a pseudo-Voigt function.

The average size of coherent scattering regions $\langle D \rangle$ was estimated by the Warren method[33] from the formula

$$\langle D \rangle = \frac{K_{hkl}\lambda}{\cos\theta\,\beta(2\theta)}, \tag{1}$$

where λ is the radiation wavelength, θ is the Bragg angle, $K_{hkl} \approx 1$ is the Scherrer constant whose value depends on the crystallite (domain) shape and reflection indices (hkl), and $\beta(2\theta) = \sqrt{(\mathrm{FWHM}_{\mathrm{exp}})^2 - (\mathrm{FWHM}_R)^2}$ is the broadening of diffraction reflection [$\mathrm{FWHM}_{\mathrm{exp}}$ being the full width of the reflection at half maximum (height) and FWHM_R the instrumental angular resolution of the diffractometer]. The angular resolution function $\mathrm{FWHM}_R(2\theta) = (u\tan^2\theta + v\tan\theta + w)^{1/2}$ of the DRON-UM1 x-ray diffractometer was determined in a special diffraction experiment with the cubic lanthanum hexaboride LaB_6 (NIST Standard Reference Powder 660a) having the lattice constant $a = 0.415\,691\,62$ nm. This angular resolution function has the following parameters: $u = 0.0041$, $v = -0.0021$, and $w = 0.0093$. Instrumental resolution functions of the $D7a$ and $D2$ neutron diffractometers were determined using a standard sample of the aluminum oxide Al_2O_3 (corundum) with the lattice constants $a = 0.4789$ nm and $c = 1.2991$ nm.

The microstructure of compact samples of the lower tungsten carbide was analyzed in reflected polarized white light under a Leica DM 2500M optical polarization microscope at a magnification of 100–1000 power. Metallographic sections were made in a Buehler metallographic installation including Pneumet-II and Motopol-8 devices. The samples were polished to the 12th class of roughness. Ready metallographic sections were etched in an acid mixture ($2HNO_3 + 6HF + 3H_2O$) so as to expose grain boundaries. The grain size in the compact carbide samples was determined by the linear-intercept method. The microhardness H_V of disordered and ordered samples of the carbide W_2C was measured by the Vickers method using a Micromet-1 testing machine with automatic loading. The load was 0.2 kg during the loading time of 10 s.

IV. SYMMETRY ANALYSIS OF POSSIBLE ORDERED PHASES IN THE LOWER TUNGSTEN CARBIDE

Disorder-order or order-order transformations, which take place with decreasing temperature, represent transitions from the state with a large free energy to the state with a smaller free energy. The state of solids during atomic or atomic-vacancy ordering can be characterized by the Landau thermodynamic potential, which in this case is the functional of probabilities of finding some species of atoms at lattice sites, coordinates of sites, and the temperature. In turn, the probabilities are the functions of the long-range order parameters η. The Landau potential has several minima, which correspond to high-symmetry disordered and low-symmetry ordered phases and depend on the crystal lattice symmetry. As the temperature decreases, the transition from the disordered phase to any of the ordered phases or from one ordered phase to another takes place only if the symmetry is reduced. The symmetry analysis provides the quantitative evaluation of the symmetry reduction after the formation of some superstructure and allows determining the physically reasonable sequence of its formation.

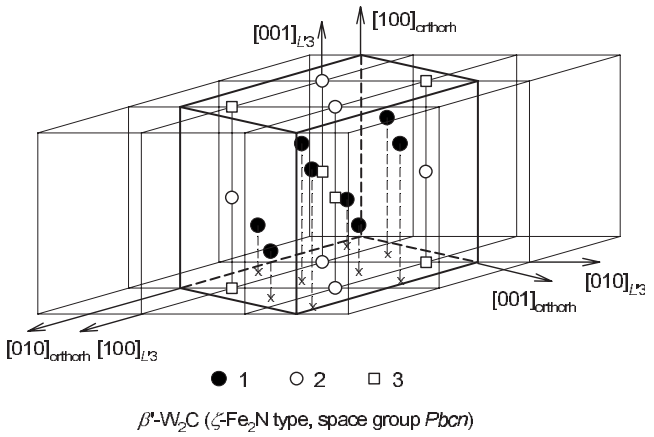

FIG. 4. Position of the unit cell of the ordered orthorhombic (space group *Pbcn*) phase β'-W_2C (ζ-W_2C) of the ζ-Fe_2N type in the basic lattice with the $L'3$ structure. (1) W atoms, (2) C atoms, and (3) vacant sites of the nonmetal sublattice.

Let us perform the symmetry analysis of possible ordered phases of the lower tungsten carbide W_2C, i.e., establish corresponding channels of the disorder-order transition, calculate the distribution functions of carbon atom, and determine the change of the symmetry upon transition from one phase to another. The procedure of calculation of the superstructure vectors of the reciprocal lattice, the disorder-order phase transition channel, and the distribution function is described in detail elsewhere.[1,2]

The high-temperature phase β-W_2C has the hexagonal structure of the $L'3$ type with a disordered arrangement of C atoms and structural vacancies $\square$ at sites $2(a)$ having the coordinates (0 0 0) and (0 0 1/2). The volume of the unit cell of β-W_2C carbide is $V=(\sqrt{3}/2)a^2c$. In the disordered lower carbide β-W_2C with the $L'3$ structure, the Ising lattice, in which atomic-vacancy ordering can take place, is the hexagonal nonmetal sublattice. In the carbide β-W_2C, the lattice constants $a_x=a_y=a$, while the lattice constant a_z of the translational primitive (concerning the nonmetal sublattice) cell in the direction [001] is twice as small as the lattice constant c of the unit cell, i.e., $a_z=c/2$ (Fig. 1). Therefore, structural vectors of the reciprocal lattice of the basic hexagonal lattice are $\mathbf{b}_1=(1,0,0)$ and $\mathbf{b}_2=(0,0,1)$ in units $4\pi/(a\sqrt{3})$, while $\mathbf{b}_3=(0,0,1)$ in units $4\pi/c$.

The assumed modification β'-W_2C with the structure of the ζ-Fe_2N type has the orthorhombic (space group *Pbcn*) symmetry, although the metal sublattice remains to be a hexagonal closely packed one similar to the lattice of the high-temperature carbide β-W_2C. In this structure, W atoms are at sites $8(d)$ with the coordinates ($\sim$1/4 $\sim$1/8 $\sim$1/12), while C atoms occupy positions $4(c)$ with the coordinates (0 $\sim$3/8 1/4). Positions $4(c)$ with the coordinates (0 $\sim$7/8 1/4) are vacant. Lattice constants of the perfect orthorhombic phase β'-W_2C are $a_{\text{orthorh}}=c_{L'3}$, $b_{\text{orthorh}}=2a_{L'3}$, and $c_{\text{orthorh}}=(\sqrt{3})a_{L'3}$, while the volume of the unit cell of this phase is $V_{\text{orthorh}}=(2\sqrt{3})a^2c$. The phase β'-W_2C (Fig. 4) is ordered by the nonmetal sublattice as compared to the high-temperature hexagonal phase β-W_2C (Fig. 1).

Calculations show that one nonequivalent superstructure vector $-(1/2\ 1/2\ -1/2)$, which corresponds to the ray $\mathbf{k}_{14}^{(3)}=-(\mathbf{b}_1+\mathbf{b}_2-\mathbf{b}_3)/2$ of the three-ray star $\{\mathbf{k}_{14}\}$, is present in the first Brillouin zone of the disordered nonmetal hexagonal sublattice when the orthorhombic phase is formed (here and henceforth the stars $\{\mathbf{k}_s\}$ of the wave vectors of the hexagonal lattice are numbered and described according to Ref. 34). Thus, the β'-W_2C (space group $P6_3/mmc$) $\rightarrow$ β'-W_2C (space group *Pbcn*) disorder-order transition channel includes one superstructure vector $\mathbf{k}_{14}^{(3)}$.

The structure of ordered phases is conveniently described by the distribution function $n(\mathbf{r})$, which is the probability that an atom of the given species is located at a site $\mathbf{r}$ of the ordering sublattice. The deviation of the probability $n(\mathbf{r})$ from its value for a disordered (statistical) distribution can be presented as a superposition of several plane concentration waves.[35] The wave vectors of these waves are superstructure vectors forming the disorder-order transition channel.[1,2] In the method of static concentration waves,[35] the distribution function $n(\mathbf{r})$ has the form

$$n(\mathbf{r}) = y + \frac{1}{2}\sum_s \sum_{j\in s} \eta_s\gamma_s[\exp(i\varphi_s^{(j)})\exp(i\mathbf{k}_s^{(j)}\mathbf{r}) + \exp(-i\varphi_s^{(j)})\exp(-i\mathbf{k}_s^{(j)}\mathbf{r})], \quad (2)$$

where y is the fraction of sites occupied by atoms of the given species in the ordering sublattice, η_s is the long-range order parameter corresponding to the star $\{\mathbf{k}_s\}$, $\mathbf{k}_s^{(j)}$ is the superstructure vector of the star $\{\mathbf{k}_s\}$ generating the concentration wave, and $\eta_s\gamma_s$ and $\varphi_s^{(j)}$ are the amplitude and the phase shift of the concentration wave, respectively.

Considering Eq. (2), the distribution function of carbon atoms in the orthorhombic (space group *Pbcn*) phase β'-W_2C depends on one long-range order parameter η_{14}, which corresponds to the star $\{\mathbf{k}_{14}\}$. In accordance with calculations, this function has the form

$$n(x_I,y_I,z_I) = y + (\eta_{14}/2)\cos\,\pi(x_I + y_I - 2z_I), \quad (3)$$

where $y \leqslant 0.5$ is the relative concentration of carbon in the carbide β'-W_2C (WC_y); x_I, y_I, and z_I are coordinates of sites $\mathbf{r}$ in the nonmetal sublattice of the basic disordered hexagonal phase. The distribution function [Eq. (3)] takes two values (Table II) at sites relating to different positions in the nonmetal sublattice of the orthorhombic β'-W_2C superstructure. Values of the distribution function at sites relating to different positions in the nonmetal sublattice of any ordered phase are the occupancy of these sites by carbon atoms or, which is the same, the probability that carbon atoms are present at these sites.

In the case of disorder-order or order-order transformations, the change of the point (rotational) symmetry N_p upon transition from phase 1 to phase 2 equals the ratio of the order of point symmetry groups of phases 1 and 2, i.e., $N_p=n_p(G_1)/n_p(G_2)$. The order $n_p(G)$ of a point symmetry group G equals the number of symmetry elements in this group. The change of the translational symmetry, N_t, is equal to the ratio between volumes V_2 and V_1 of the unit cells of phases 2 and 1 or the ratio of the number of crystallographic sites m_2 and m_1 in the unit cells of these phases, i.e., $N_t=V_2/V_1\equiv m_2/m_1$. The total change of the symmetry N

TABLE II. Orthorhombic [ζ-Fe_2N type, Space Group No. 60, $Pbcn$ (D_{2h}^{14})] ordered phase β'-W_2C (ζ-W_2C), $Z=4$: $\mathbf{a}_{\text{orthorh}}=\langle 001\rangle_{L'3}$, $\mathbf{b}_{\text{orthorh}}=2\langle 100\rangle_{L'3}$, $\mathbf{c}_{\text{orthorh}}=\langle 120\rangle_{L'3}$.

Atom	Position and multiplicity	Atomic coordinates in the basic disordered structure			Atomic coordinates in the ideal ordered structure			Values for the distribution function
		$x_I=x/a_{L'3}$	$y_I=y/b_{L'3}$	$z_I=z/c_{L'3}$	x/a_{orthorh}	y/b_{orthorh}	z/c_{orthorh}	$n(x_I,y_I,z_I)$
C1 (vacancy)	4(c)	1	0	0	0	7/8	1/4	$n_1=y-\eta_{14}/2$
C2	4(c)	0	0	0	0	3/8	1/4	$n_2=y+\eta_{14}/2$
W	8(d)	−2/3	−1/3	1/4	1/4	1/8	1/12	

upon transition from phase 1 to phase 2 equals the product of the change of the point symmetry N_p by the change of the translational symmetry N_t, i.e., $N=N_pN_t=n_p(G_1)V_2/n_p(G_2)/V_1\equiv[n_p(G_1)/V_1]/(n_p(G_2)/V_2)$.

The point symmetry group mmm (D_{2h}) of the orthorhombic carbide β'-W_2C includes 8 symmetry elements H_1, H_4, H_7, H_9, H_{13}, H_{16}, H_{19}, and H_{21}, while the point group $6/mmm$ (D_{6h}) of the basic (parent) disordered phase β-W_2C has 24 elements H_1-H_{24}.[1,2,34] Therefore, the point (rotational) symmetry reduction N_p equals 3. When going from the disordered carbide β-W_2C to the orthorhombic carbide β'-W_2C, the unit cell volume increases by a factor of 4 and, hence, the translational symmetry reduction N_t is equal to 4. Therefore, the total symmetry reduction is $N=N_pN_t=12$ upon the β-W_2C (space group $P6_3/mmc$)$\rightarrow\beta'$-W_2C (space group $Pbcn$) transition.

Translation vectors of the unit cell of the rhombohedral (space group $P\bar{3}m1$) phase β''-W_2C with the structure of the $C6$ type coincide with translation vectors of the unit cell of the disordered hexagonal phase (Fig. 5) and are equal to $\mathbf{a}_{C6}=(100)_{L'3}$, $\mathbf{b}_{C6}=[010]_{L'3}$, and $\mathbf{c}_{C6}=[001]_{L'3}$. Therefore, the volume of the unit cell of the rhombohedral phase

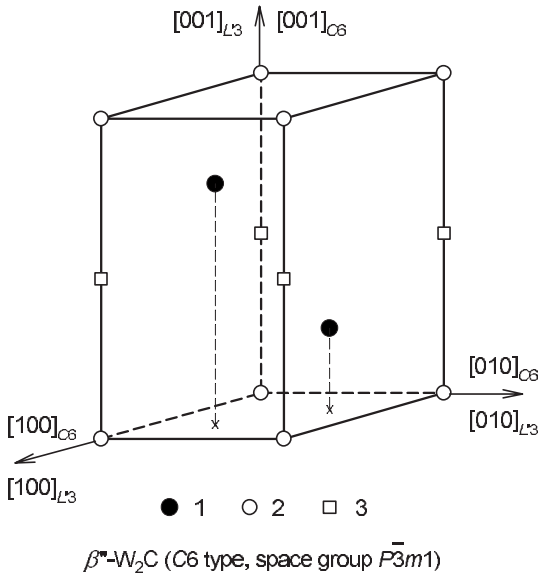

FIG. 5. Position of the unit cell of the ordered rhombohedral (space group $P\bar{3}m1$) phase β''-W_2C of the $C6$ type in the basic lattice with the $L'3$ structure. (1) W atoms, (2) C atoms, and (3) vacant sites of the nonmetal sublattice.

$V_{C6}=(\sqrt{3}/2)a^2c$ equals the volume of the unit cell of the disordered carbide β-W_2C. In an ideal case, two W atoms occupy positions 2(d) with the coordinates (1/3 2/3 z) and (2/3 1/3 $-z$), where $z=0.25$, the C atom is in the position 1(a) with the coordinates (0 0 0), and the vacant site is in the position 1(b) with the coordinates (0 0 1/2) in the phase β''-W_2C. The comparison with the disordered carbide β-W_2C (Fig. 1) clearly shows that the positions 2(a), which are statistically half-filled with C atoms, split to positions 1(a) and 1(b) (one position being occupied by carbon atoms, while the other being vacant) as a result of rhombohedral ordering.

According to calculations, the phase β''-W_2C is formed by the disorder-order transition channel including the ray $\mathbf{k}_{17}^{(1)}=\mathbf{b}_3/2$ of the star $\{\mathbf{k}_{17}\}$. Therefore, the carbon atom distribution function at sites $\mathbf{r}$ in the nonmetal sublattice of the ordered rhombohedral phase β''-W_2C (WC_y) with any degree of order has the form

$$n(x_I,y_I,z_I)=y+(\eta_{17}/2)\cos 2\pi z_I \tag{4}$$

and depends on one long-range order parameter η_{17}. Values of the distribution function [Eq. (4)] at sites in the nonmetal sublattice of the rhombohedral superstructure are given in Table III.

The point symmetry group $\bar{3}m$ (D_{3d}) of the rhombohedral carbide β''-W_2C includes 12 symmetry elements[1,2,33] H_1, H_3, H_5, H_8, H_{10}, H_{12}, H_{13}, H_{15}, H_{17}, H_{20}, H_{22}, and H_{24} out of 24 elements of the hexagonal group $6/mmm$. Therefore, the rotational symmetry reduction is $N_p=2$. Since the unit cell volume does not change in going from the disordered to the ordered state, the translational symmetry reduction is 1, while the total symmetry reduction upon the β-W_2C (space group $P6_3/mmc$)$\rightarrow\beta''$-W_2C (space group $P\bar{3}m1$) transformation equals 2.

The trigonal (space group $P\bar{3}1m$) phase ε-W_2C has the unit cell (Fig. 6) with translation vectors $\mathbf{a}_\varepsilon=[1-10]_{L'3}$, $\mathbf{b}_\varepsilon=[120]_{L'3}$, and $\mathbf{c}_\varepsilon=[001]_{L'3}$ and the volume $V_\varepsilon=(3\sqrt{3}/2)a^2c$. In the perfect trigonal superstructure, W atoms occupy positions 6(k) with the coordinates (1/3 0 1/4), and C atoms are at sites 1(a) with the coordinates (0 0 0) and 2(d) with the coordinates (1/3 2/3 1/2), whereas site 1(b) with the coordinates (0 0 1/2) and sites (2(c) with the coordinates (1/3 2/3 0) are vacant.

Calculations of the superstructure vectors of the reciprocal lattice of the trigonal phase ε-W_2C and their translation

TABLE III. Rhombohedral [C6 type (anti-CdI_2), Space Group No. 164, $P\bar{3}m1$ (D_{3d}^3)] ordered phase β''-W_2C, $Z=1$: $\mathbf{a}_{C6}=\langle 100\rangle_{L'3}$, $\mathbf{b}_{C6}=\langle 010\rangle_{L'3}$, $\mathbf{c}_{C6}=\langle 001\rangle_{L'3}$.

Atom	Position and multiplicity	Atomic coordinates in the ideal ordered structure			Values for the distribution function
		$x/a_{C6}\equiv x/a_{L'3}$	$y/b_{C6}\equiv y/b_{L'3}$	$z/c_{C6}\equiv z/c_{L'3}$	$n(x_I,y_I,z_I)$
C1 (vacancy)	1(*b*)	0	0	1/2	$n_1=y-\eta_{17}/2$
C2	1(*a*)	0	0	0	$n_2=y+\eta_{17}/2$
W	2(*d*)	1/3	2/3	1/4	

show that three nonequivalent superstructure vectors are present in the first Brillouin zone of the disordered nonmetal hexagonal sublattice. The first vector corresponds to the ray $\mathbf{k}_{17}^{(1)}=\mathbf{b}_3/2$ of the Lifschitz one-ray star $\{\mathbf{k}_{17}\}$, while the other two vectors correspond to the rays $\mathbf{k}_{15}^{(1)}=(\mathbf{b}_1+\mathbf{b}_2)/3+\mathbf{b}_3/2$ and $\mathbf{k}_{15}^{(2)}=-\mathbf{k}_{15}^{(1)}$ of the Lifschitz two-ray star $\{\mathbf{k}_{15}\}$. Thus, the disorder-order phase transition channel, which is connected with the formation of the ordered trigonal phase ε-W_2C, includes three superstructure vectors $\mathbf{k}_{15}^{(1)}$, $\mathbf{k}_{15}^{(2)}$, and $\mathbf{k}_{17}^{(1)}$. The presence of Lifschitz star rays alone in the transition channel means that the formation of the trigonal superstructure satisfies the Landau criterion for second-order phase transitions. This is in agreement with results of Refs. 20 and 23, in which the β-$W_2C\leftrightarrow\varepsilon$-$W_2C$ disorder-order transformation is a second-order phase transition. However, the fulfillment of the Landau criterion does not exclude the possibility that the β-$W_2C\leftrightarrow\varepsilon$-$W_2C$ transformation is realized by the mechanism of the first-order phase transition.

The carbon atom distribution function for the ordered trigonal phase ε-W_2C_y (WC_y, $y\leqslant 0.5$) has the form

$$n(x_I,y_I,z_I)=y-(\eta_{17}/6)\cos 2\pi z_I+(2\eta_{15}/3)\times\cos[(2\pi/3)(x_I+y_I+3z_I)]. \quad (5)$$

This function depends on two long-range order parameters

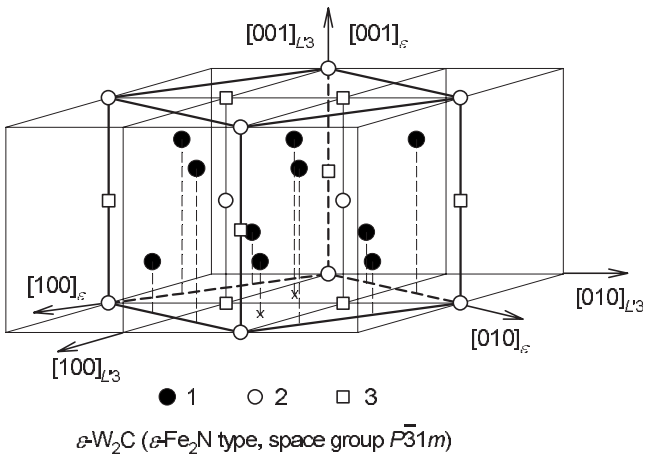

FIG. 6. Position of the unit cell of the ordered trigonal (space group $P\bar{3}1m$) phase ε-W_2C of the ε-Fe_2N type in the basic lattice with the $L'3$ structure. (1) W atoms, (2) C atoms, and (3) vacant sites of the nonmetal sublattice.

η_{17} and η_{15} corresponding to the stars $\{\mathbf{k}_{17}\}$ and $\{\mathbf{k}_{15}\}$. It takes four values (Table IV) at sites in the nonmetal sublattice of the trigonal phase ε-W_2C.

The ray $\mathbf{k}_{17}^{(1)}$ of the star $\{\mathbf{k}_{17}\}$ and the long-range order parameter η_{17} determine the alternation of nonmetal atomic planes $(00z)_\varepsilon$, which are perpendicular to the c axis and differ in the occupancy by C atoms: the planes $(00z)_\varepsilon$ with occupancies 1/3 (at $z=0$) and 2/3 (at $z=1/2$) alternate in the perfect ordered phase ε-W_2C (Fig. 6). The rays $\mathbf{k}_{15}^{(1)}$ and $\mathbf{k}_{15}^{(2)}$ of the star $\{\mathbf{k}_{15}\}$ and the long-range order parameter η_{15} determine the location of C atoms and vacancies $\square$ in nonmetal planes $(00z)_\varepsilon$.

The rotational symmetry reduction N_p is 2 and the unit cell volume increases by a factor of 3 upon the β-W_2C (space group $P6_3/mmc$)$\rightarrow\varepsilon$-W_2C (space group $P\bar{3}1m$) transition. Taking this into account, when going from the disordered carbide β-W_2C to the trigonal carbide ε-W_2C, the total symmetry reduction $N=N_pN_t$ is equal to 6.

The change of the symmetry during the formation of possible orthorhombic and rhombohedral phases is such that the sequence of disordered hexagonal phase β-$W_2C\rightarrow$ordered orthorhombic phase β'-$W_2C\rightarrow$ordered rhombohedral phase β''-W_2C transformations, which is proposed in Refs. 9 and 11, is physically impossible because the symmetry increases rather than decreases during the β'-$W_2C\rightarrow\beta''$-W_2C transition.

If all the three superstructures are formed at different stages of ordering of carbide W_2C, the symmetry analysis suggests the only possible sequence of phase transformations, which take place with decreasing temperature and do not contradict the symmetry variation: disordered hexagonal (space group $P6_3/mmc$) phase β-$W_2C\rightarrow$ordered rhombohedral (space group $P\bar{3}m1$) phase β''-$W_2C\rightarrow$ordered trigonal (space group $P\bar{3}1m$) phase ε-$W_2C\rightarrow$ordered orthorhombic (space group $Pbcn$) phase β'-W_2C. In this case, the symmetry is reduced twice on the transition from the disordered hexagonal to the rhombohedral carbide, then thrice on the transition from the rhombohedral to the trigonal carbide, and finally twice on the transition from the trigonal to the orthorhombic carbide. If some ordered phase is not detected in the experiment, the transformation sequence is still physically correct even without this phase.

Considering the above analysis, let us discuss the results of the experimental research into the structure of the lower tungsten carbide W_2C.

TABLE IV. Ideal trigonal [ε-Fe_2N type, Space Group No. 162, $P\bar{3}1m$ (D^1_{3d})] ordered phase ε-W_2C, $Z=3$: $\mathbf{a}_\varepsilon=\langle 1-10\rangle_{L'3}$, $\mathbf{b}_\varepsilon=\langle 120\rangle_{L'3}$, $\mathbf{c}_\varepsilon=\langle 001\rangle_{L'3}$.

Atom	Position and multiplicity	Atomic coordinates in the basic disordered structure			Atomic coordinates in the ideal ordered structure			Values for the distribution function $n(x_I,y_I,z_I)$
		$x_I=x/a_{L'3}$	$y_I=y/b_{L'3}$	$z_I=z/c_{L'3}$	x/a_ε	y/b_ε	z/c_ε	
C1 (vacancy)	1(b)	0	0	1/2	0	0	1/2	$n_1=y+\eta_{17}/6-2\eta_{15}/3$
C2 (vacancy)	2(c)	1	1	0	1/3	2/3	0	$n_2=y-\eta_{17}/6-\eta_{15}/3$
C3	1(a)	0	0	0	0	0	0	$n_3=y-\eta_{17}/6+2\eta_{15}/3$
C4	2(d)	1	1	1/2	1/3	2/3	1/2	$n_4=y+\eta_{17}/6+\eta_{15}/3$
W	6(k)	1/3	−1/3	1/4	1/3	0	1/4	

V. REAL STRUCTURE OF ORDERED PHASE IN LOWER TUNGSTEN CARBIDE

The x-ray diffraction (XRD) pattern of powder, produced by plasma chemical synthesis, contains diffraction reflections of three phases: the lower W_2C and the higher WC tungsten carbide, and tungsten W. All the reflections are very broad. Broadening is due to a small size of particles of the synthesized powder. The average size of coherent scattering regions was 55±10 nm as estimated from diffraction reflection broadening. Minimization of the XRD pattern showed that the nanocrystalline sample contains ~75 wt % W_2C (space group $P6_3/mmc$), ~15 wt % W, and ~10 wt % WC. Under these conditions, the reliability factor R_I (R_{Bragg}) is 0.135. Taking into account the presence of ordered phases (ε-W_2C, β'-W_2C, or β''-W_2C) did not improve convergence because of the large broadening of the diffraction reflections. The unit cell lattice constants for the disordered carbide W_2C are equal to $a_{L'3}=0.3027$ and $c_{L'3}=0.4766$ nm. The unit cell lattice constant a in the metallic tungsten is 0.3158 nm. The lattice constants of the unit cell of tungsten monocarbide WC are $a=0.2896$ and $c=0.2865$ nm.

The chemical analysis showed that the total content of carbon in the nanopowder is ~6.2 wt % including ~3.6 wt % free amorphous carbon. According to results of the XRD and the chemical analysis, the nanocrystalline powder contains ~72.5 wt % W_2C, ~14.5 wt % W, ~9.5 wt % WC, and ~3.5 wt % C.

The nanocrystalline powder was studied by neutron diffraction using neutrons of wavelengths of 0.1532 and 0.1805 nm. Measurements with neutrons having the large wavelength were made for a more detailed analysis of the small-angle scattering region, which could contain reflections characteristic of some ordered phase. Neutron diffraction patterns of the nanocrystalline powder are given in Fig. 7.

Neutron diffraction patterns of the nanocrystalline powder under radiation with $\lambda=0.1532$ were taken over the interval of interplanar spacings $0.9\geqslant d\geqslant 0.09$ nm. Measurements under long-wave radiation with $\lambda=0.1805$ nm covered a wider interval of $1.7\geqslant d\geqslant 0.1$ nm. At $2\theta<32°$, both neutron diffraction patterns clearly exhibit the superstructure reflection $(011)_\varepsilon$ with $d\approx 0.3304$ nm, which is characteristic of the ordered carbide ε-W_2C (Fig. 7). Both neutron diffraction patterns contain the same set of diffraction reflections of four

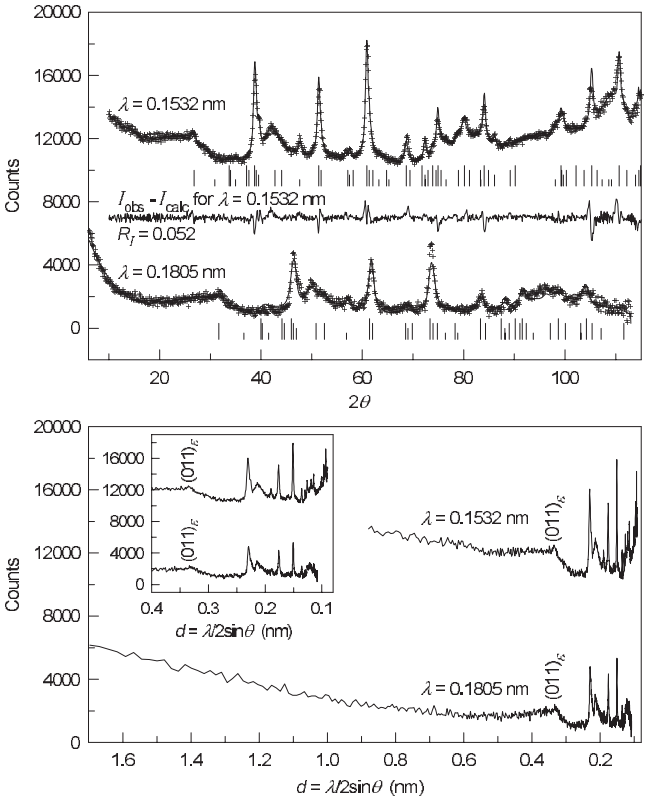

FIG. 7. Experimental (crosses) and calculated (solid line) neutron diffraction patterns ($\lambda=0.1532$ and 0.1805 nm) of the nanocrystalline powder containing ~65.0 wt % disordered lower tungsten carbide W_2C, ~9.5 wt % ordered trigonal (space group $P\bar{3}1m$) carbide ε-W_2C, ~14.0 wt % W, ~8.0 wt % WC, and ~3.5 wt % free amorphous carbon C. Difference neutron diffraction pattern is shown for neutrons of wavelength of 0.1532 nm only. For comparison, the experimental neutron diffraction patterns are shown as a function of the interplanar spacing $d=\lambda/(2\sin\theta)$. The inset presents the neutron diffraction patterns in the interval $0.5>d>0.08$ nm. At $2\theta<32°$, both neutron diffraction patterns clearly exhibit the superstructure reflection $(011)_\varepsilon$ with $d\approx 0.3304$ nm, which is characteristic of the ordered trigonal carbide ε-W_2C. The longest ticks denote diffraction reflections of the disordered phase W_2C; long, medium, and short ticks correspond to reflections of ε-W_2C, W, and WC, respectively.

phases: the disordered lower hexagonal (space group $P6_3/mmc$) tungsten carbide W_2C, the ordered trigonal (space group $P\bar{3}1m$) carbide ε-W_2C, metallic tungsten W with the bcc (space group $Im\bar{3}m$) structure, and the hexagonal (space group $P\bar{6}m2$) monocarbide WC. Reflections of the ordered orthorhombic (space group $Pbcn$) and rhombohedral (space group $P\bar{3}m1$) carbides β'-W_2C and β''-W_2C are not detected.

A neutron diffraction pattern, which was collected with a large signal accumulation under radiation with $\lambda=0.1532$ nm, was used for a more detailed analysis of the structure of the observed phases. According to calculations, the concentrations of the detected crystal phases in the nanocrystalline powder are ~67.5 wt % W_2C, ~9.8 wt % ε-W_2C, ~14.5 wt% W, and ~8.2 wt % WC. Taking into account the presence of free carbon in the nanopowder, the phase concentration is ~65.0 wt % W_2C, ~9.5 wt % ε-W_2C, ~14.0 wt % W, ~8.0 wt % WC, and ~3.5 wt % C. These values are in agreement with the data obtained by minimization of the XRD pattern of the same powder. A comparatively small concentration of the ordered carbide ε-W_2C and a large (~65.0 wt %) concentration of the disordered carbide W_2C in the nanocrystalline powder are explained by quenching of the nanopowder from a high temperature of ~2400 K. The multiple phases of the nanocrystalline powder result from the fact that the plasma chemical synthesis reaction is realized far from equilibrium conditions.

The neutron diffraction pattern was used for the structure refinement by the GSAS program.[32] It was established that the unit cell lattice constants in the tungsten monocarbide WC are equal to $a=0.2893(8)$ nm and $c=0.2818(9)$ nm, while the unit cell lattice constant in metallic tungsten is 0.3155(2) nm. As for the lower tungsten carbide W_2C, $a_{L'3}=0.299\,47(6)$ nm and $c_{L'3}=0.4728(1)$ nm for the disordered phase. These lattice constants correspond to carbide ~$WC_{0.46}$. The lattice constants and the volume of the unit cell in the ordered phase ε-W_2C are equal to $a_\varepsilon=0.5152(6)$ nm, $c_\varepsilon=0.4681(2)$ nm, and $V_\varepsilon=107.568\times10^{-3}$ nm^3. Thus, the lattice constants a_ε and c_ε are smaller than the theoretical values of these constants $a_{\varepsilon\text{theor}}=a_{L'3}\sqrt{3}$ and $c_{\varepsilon\text{theor}}=c_{L'3}$ in the perfect ordered phase. Minimization of the neutron diffraction pattern taking into account the ordered phase ε-W_2C with a fixed occupancy of sites equal to their occupancy in the perfect trigonal superstructure provides satisfactory agreement of the calculated and experimental spectra: the factor $R_I=0.052$. Varying of the occupancy of sites in the trigonal superstructure did not lead to considerable improvement of the agreement between the experimental and calculated neutron diffraction patterns because of multiple phases of the sample, large broadening of diffraction reflections, and a small content of the ordered carbide ε-W_2C. The reliability factor R_I equals 0.083 for the neutron diffraction pattern ($\lambda=0.1805$ nm) collected with a small signal accumulation.

To determine the temperature range of existence of the lower tungsten carbide W_2C and the ordered phase ε-W_2C, samples of the lower tungsten carbide were synthesized additionally by solid-phase sintering of W and C powders at temperatures of ~2070 and 1370 K. The neutron diffraction pattern of the lower carbide W_2C, which was synthesized at 2070 K for 10 h, is shown in Fig. 8.

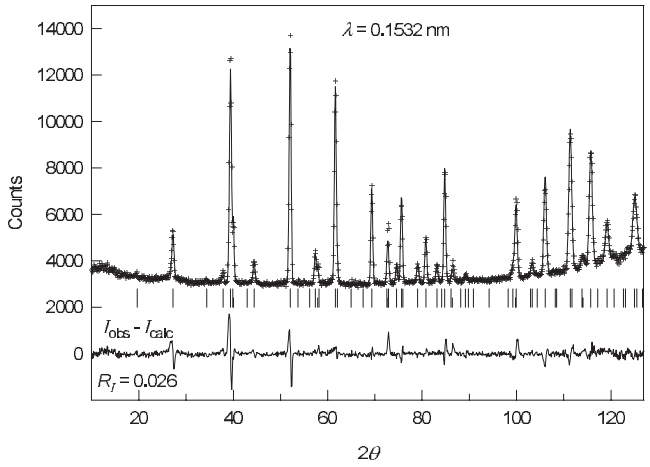

FIG. 8. Experimental (crosses), calculated (solid line), and difference neutron diffraction patterns ($\lambda=0.1532$ nm) of the lower carbide W_2C synthesized by sintering of W+C powdered mixture at 2070 K for 10 h. The long and short ticks correspond to reflections of the ordered phase ε-W_2C and tungsten W.

The neutron diffraction pattern (Fig. 8) contains a set of diffraction reflections, which is characteristic of the ordered trigonal (space group $P\bar{3}1m$) phase ε-W_2C. Also, reflections of cubic (space group $Im\bar{3}m$) tungsten with the lattice constant $a=0.316\,51(1)$ nm are observed. The best agreement between the experimental and theoretical spectra ($R_I=0.0258$, $R_p=0.0353$, $\omega R_p=0.0448$) was achieved by taking into account different occupancies of sites by C atoms in the nonmetal sublattice (Table V). The occupancy of the sites $1(a)$ and $2(d)$ proved to be less than 1, whereas a small number of carbon atoms occupied the sites $1(b)$ and $1(c)$, which are fully vacant in the perfect ordered phase. The occupancies of sites in the nonmetal sublattice differ from the ideal values of 1 and 0. It is explained both by the deviation of the composition of the ordered carbide from the stoichiometric composition W_2C and by the fact that the degree of the long-range order in the carbide is less than the maximum one.

The relative concentration of carbon in the ordered trigonal phase indeed equals $y=(n_1+2n_2+n_3+2n_4)/6$, where n_1, n_2, n_3, and n_4 denote occupancies of nonmetal sublattice sites located in positions $1(b)$, $2(c)$, $1(a)$, and $2(d)$, respectively (see Tables IV and V). Considering the occupancy of these positions (Table V), the ordered trigonal phase ε-W_2C under study has the composition $W_2C_{0.953}$ ($WC_{0.48}$). Values of the long-range order parameters η_{17} and η_{15} can be determined from the occupancies considering values taken by the distribution function that describes the trigonal superstructure ε-W_2C,

TABLE V. Real structure of trigonal [ε-Fe_2N type, Space Group No. 162, $P\bar{3}1m$ (D^1_{3d})] ordered carbide ε-W_2C_y (Z=3) before and after annealing.

		Carbide ε-W_2C_y obtained by sintering for 10 h at a temperature of 2070 K[a] [$W_2C_{0.953}$, $a_\varepsilon=b_\varepsilon=0.51813(3)$ nm, $c_\varepsilon=0.47283(8)$ nm, $V_\varepsilon=109.932\times10^{-3}$ nm^3]					The same carbide ε-W_2C_y after annealing for 35 h at a temperature of 1370 K[a] [$W_2C_{1.00}$, $a_\varepsilon=b_\varepsilon=0.51880(2)$ nm, $c_\varepsilon=0.47273(5)$ nm, $V_\varepsilon=110.192\times10^{-3}$ nm^3]				
Atom	Position and multiplicity	Atomic coordinates in the ordered structure			B_{iso} (pm^2)	Occupancy	Atomic coordinates in the ordered structure			B_{iso} (pm^2)	Occupancy
		x/a_ε	y/b_ε	z/c_ε			x/a_ε	y/b_ε	z/c_ε		
C1 (vacancy)	1(b)	0	0	1/2	380	0.0175	0	0	1/2	0	0
C2 (vacancy)	2(c)	1/3	2/3	0	1330	0.2656	1/3	2/3	0	1120	0.2316
C3	1(a)	0	0	0	1150	0.7983	0	0	0	1280	0.7253
C4	2(d)	1/3	2/3	1/2	1030	0.7565	1/3	2/3	1/2	910	0.9093
W	6(k)	0.328(1)	0	0.253(5)	980	1	0.331(7)	0	0.252(4)	840	1

[a]The final values of reliability factors R_I, R_p, and ωR_p are given in text.

$$\eta_{15}=(n_3+n_4-n_1-n_2)/2, \quad \eta_{17}=n_1+2n_4-2n_2-n_3. \tag{6}$$

According to the estimates, the long-range order parameters in the ordered trigonal carbide ε-$W_2C_{0.953}$ ($WC_{0.48}$), which was synthesized at ~2070 K, are $\eta_{15}=0.636$ and $\eta_{17}=0.201$. The lattice constants and the volume of the unit cell in this carbide ε-W_2C are equal to $a_\varepsilon=b_\varepsilon=0.518\,13$ nm, $c_\varepsilon=0.472\,84$ nm, and $V_\varepsilon=109.932\times10^{-3}$nm^3, i.e., are larger than lattice constants a_ε and c_ε and the volume of the unit cell of the same ordered phase in the nanocrystalline powder.

The W_2C sample synthesized at 2070 K for 10 h was annealed additionally at a temperature of 1370 K for 35 h. The x-ray (Fig. 9) and neutron (Fig. 10) diffraction patterns of the annealed sample exhibit the same set of diffraction reflections of only two phases ε-W_2C and W as in the neutron diffraction pattern of the unannealed sample (see Fig. 8). The annealed and synthesized samples have the same phase composition within the calculation error and contain ~85±2 wt % ε-W_2C and ~15±2 wt % W. Refinement of the structure of the ordered phase in the annealed sample showed that the best agreement of the experimental and theoretical neutron diffraction patterns ($R_I=0.0252$, $R_p=0.0299$, $\omega R_p=0.0390$) is achieved when the carbon atom occupancy of vacancy positions 1(b) and 2(c) decreases and the occupancy of position 2(d) increases considerably (Table V). Annealing changes the ordered phase composition from ε-$W_2C_{0.953}$ ($WC_{0.48}$) to ε-$W_2C_{1.00}$ ($WC_{0.50}$). The long-range order parameters of the trigonal carbide ε-$W_2C_{1.00}$ increase to $\eta_{15}=0.702$ and $\eta_{17}=0.630$ after annealing. The lattice constants and the volume of the unit cell of the annealed carbide ε-W_2C equal $a_\varepsilon=b_\varepsilon=0.518\,80(2)$ nm, $c_\varepsilon=0.472\,73(5)$ nm, and $V_\varepsilon=110.192\times10^{-3}$ nm^3, i.e., are larger than those of the same ordered phase before annealing. The lattice constants increase because the carbon concentra-

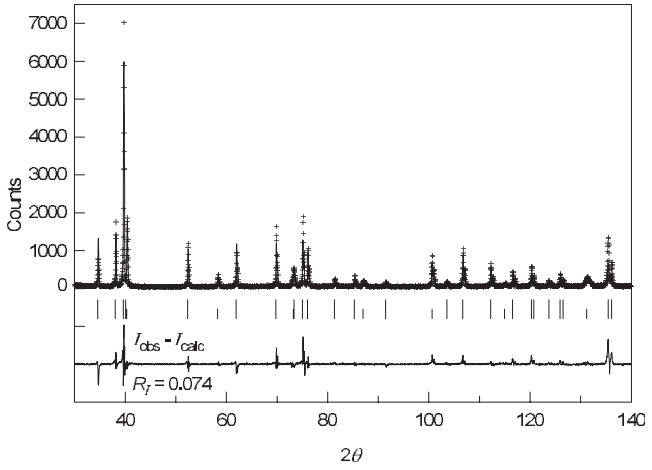

FIG. 9. Experimental (crosses), calculated (solid line), and difference XRD patterns of the lower carbide W_2C after additional annealing at 1370 K for 35 h. The long and short ticks correspond to reflections of the ordered phase ε-W_2C and tungsten W. Cu $K\alpha_{1,2}$ radiation.

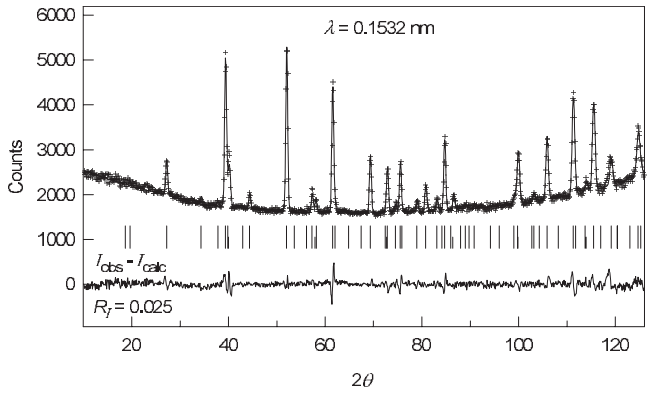

FIG. 10. Experimental (crosses), calculated (solid line), and difference neutron diffraction patterns (λ=0.1532 nm) of the lower carbide W_2C after additional annealing at 1370 K for 35 h. The long and short ticks correspond to reflections of the ordered phase ε-W_2C and tungsten W.

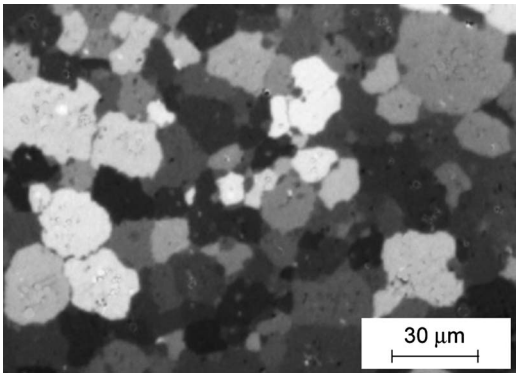

FIG. 11. Microstructure of the W_2C ($WC_{0.50}$) sample synthesized by sintering of a W+C powdered mixture at 2070 K for 10 h and subsequent annealing at 1370 K for 35 h. The size of carbide grains is 5–25 μm.

tion of the ordered trigonal carbide changes from $WC_{0.48}$ to $WC_{0.50}$.

The full width at half maximum (FWHM) of the diffraction reflections in x-ray and neutron diffraction patterns of the sintered samples of the lower tungsten carbide is not larger than the instrumental width of the corresponding reflections. The absence of broadening means that the size of grains of the ordered phase ε-W_2C in the sintered samples is larger than 200–300 nm.[36,37] We failed in observing the boundaries of domains of the ordered trigonal phase ε-W_2C by optical polarization microscopy; therefore, the domain size was supposed to be less than 1 μm. It may be assumed therefore that the size of domains of the ε-W_2C phase in the sintered samples is $0.3<\langle D\rangle<1.0$ μm. According to microscopy observations, the size of carbide grains in the sintered polycrystalline samples of W_2C is 5–25 μm (Fig. 11). The grains have an irregular prismatic shape characteristic of crystals of the hexagonal or the trigonal system. The examination of the microstructure of the sintered samples in reflected polarized white light showed that all carbide grains have an interference color, i.e., are anisotropic. When nonstoichiometric carbides are ordered by the mechanism of the first-order phase transition (e.g., ordering in titanium TiC_y and vanadium VC_y carbides[38,39]), the optical microscopy easily reveals interfaces between the disordered and ordered phases even if the size of domains of the ordered phase is small (100 nm or smaller). According to diffraction data, the disordered phase is absent in the sintered W_2C samples before and after annealing. As for the ordered phase, the degree of the long-range order in this phase increases after annealing. The presence of the ordered carbide phase alone is in agreement with the relevant microscopy observations, which did not reveal interfaces between the disordered and ordered phases. In turn, the absence of interfaces means that the formation of the trigonal phase ε-W_2C is realized most likely as the second-order phase transition. The symmetry analysis also suggests the possibility of the β-W_2C (space group $P6_3/mmc$) $\rightarrow$ ε-W_2C (space group $P\bar{3}1m$) disorder-order transition of the second order. At the same time, the formation of the trigonal phase ε-W_2C is connected with two wave-vector stars. The simultaneous distortion of the symmetry by two stars and the presence of the disordered β-W_2C and ordered ε-W_2C phases in the plasma chemical nanopowder do not exclude the possibility of the first-order phase transition. The measured microhardness of the annealed W_2C sample, which contained the ordered trigonal carbide ε-W_2C, was $H_V=15.3\pm0.3$ GPa (1560 ± 30 kg/mm^2). According to the literature data, the microhardness of the lower tungsten carbide in an unknown structural state is 14.5–18.1 GPa.

As noted above, nonmetal atomic planes $(00z)_\varepsilon$ with $z=0$ and $z=1/2$, which differ in their carbon atom occupancies, alternate at the right angle to the direction $[001]_\varepsilon$ in the ordered trigonal carbide (see Fig. 6). The probabilities that a carbon atom is located in these planes are $n_{z=0}=(2n_2+n_3)/3$ and $n_{z=1/2}=(n_1+2n_4)/3$. These probabilities are equal to 1/2 in the disordered basic hexagonal phase β-W_2C. In the perfect ordered phase ε-W_2C, probabilities are $n_{z=0}=1/3$ and $n_{z=1/2}=2/3$. In turn, they are $n_{z=0}=0.443$ and $n_{z=1/2}=0.510$ in the carbide ε-$W_2C_{0.953}$ synthesized at ~2070 K. When this carbide was annealed additionally at a temperature of ~1370 K for 35 h, the long-range order parameters η_{15} and η_{17} increased and the probabilities $n_{z=0}$ and $n_{z=1/2}$ reached 0.396 and 0.606, which are close to the values of $n_{z=0}$ and $n_{z=1/2}$ in the perfect ordered phase ε-W_2C. The comparison of the values of $n_{z=0}$ and $n_{z=1/2}$ shows that carbon atoms are redistributed between adjacent nonmetal atomic planes $(00z)_\varepsilon$ with $z=0$ and $z=1/2$ during trigonal ordering in the lower tungsten carbide.

An analysis of the calculated distribution functions allows us to establish the relationship between the maximum value of the long-range order parameter and the composition of the nonstoichiometric carbide $W_2C_y \equiv WC_y$ ($y\leqslant 0.5$). This relationship has the form

$$\eta^{\max}(y)=\begin{cases}2(1-y) & \text{if } y\geqslant 0.5\\ 2y & \text{if } y<0.5.\end{cases} \tag{7}$$

The dependence of the maximum value of any long-range order parameter on the composition of the carbide WC_y, which is ordered after the W_2C type, is defined by Eq. (7) and the minimum value of the long-range order parameters is zero. Therefore, any order parameter η describing the above superstructures meets the condition

$$0\leqslant \eta_s \leqslant m^*, \tag{8}$$

where $m^*=2(1-y)$ if $y\geqslant 0.5$ and $m^*=2y$ if $y<0.5$.

Condition (8) uniquely defines one-dimensional intervals of admissible values of the long-range order parameters for superstructures which are described by one parameter η_s. The ordered trigonal phase ε-W_2C is described by the distribution function [Eq. (5)], which depends on two long-range order parameters η_{17} and η_{15}. In the case of superstructures described by several long-range order parameters, one should be careful that the distribution function values always fall within 0 and 1. Taking into account values of the distribution function (Table IV) and the aforementioned constraints, the interval of admissible values of long-range order parameters $\eta_{17}(y)$ and $\eta_{15}(y)$ for the ordered trigonal (space group $P\bar{3}1m$) phase ε-W_2C is defined by the conditions

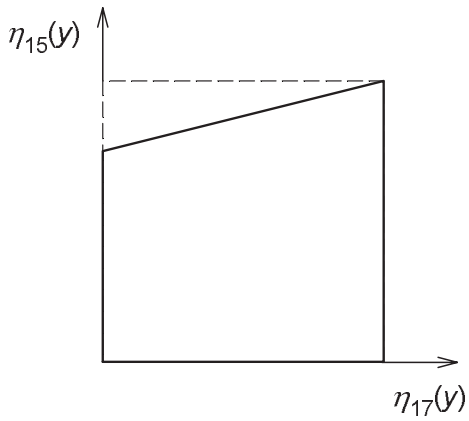

FIG. 12. Two-dimensional interval of admissible values of the long-range order parameters η_{17} and η_{15} for the ordered trigonal (space group $P\bar{3}1m$) tungsten carbide ε-W_2C.

$$-m^* \leqslant -\eta_{17}(y) + 4\eta_{15}(y) \leqslant 3m^*,$$

$$0 \leqslant \eta_{17}(y) \leqslant m^*. \quad (9)$$

The interval of admissible values of the order parameters $\eta_{17}(y)$ and $\eta_{15}(y)$ for the ordered trigonal phase ε-W_2C is shown in Fig. 12.

The distribution function [Eq. (5)] describing the ordered phase ε-W_2C is a superposition of two concentration waves related to the long-range order parameters η_{17} and η_{15}. Figure 13 presents the superposition of these concentration waves calculated for the plane $(1-1\ 1)_{L'3}$ taking some admissible values of the parameters η_{17} and η_{15}.

VI. LOW-TEMPERATURE LIMIT OF W_2C EXISTENCE RANGE

The x-ray and neutron diffraction analyses of the phase composition and the structure showed that the W_2C sample synthesized at ~2070 K and the same sample, which was annealed additionally at a temperature of 1370 K for 35 h, contain only the ordered trigonal carbide ε-W_2C and tungsten W (see Figs. 8–10). The concentrations of these phases in the sample before and after annealing are nearly equal, but the degree of order in the trigonal carbide ε-W_2C increases after annealing. Rudy,[11] Kublii and Velikanova,[27] and Gleiser and Chipman[28] think that W_2C decomposes to W and WC at temperatures of 1530 K and lower. According to Ref. 27, the ordered orthorhombic (space group *Pbcn*) phase β'-W_2C is formed as an intermediate product of decomposition. If decomposition occurs, annealing of the W_2C sample at 1370 K (150 K below the temperature of the supposed solid-phase decomposition) for 35 h should lead to the formation of the higher carbide WC. However, the x-ray and neutron diffraction analyses did not reveal any traces of WC in the sample. Diffraction reflections of the ordered orthorhombic (space group *Pbcn*) phase β'-W_2C were not observed either. The absence of reflections of the orthorhombic (space group *Pbcn*) phase β'-W_2C in the neutron diffraction pattern is in agreement with the results.[15,16,20] According to these data,

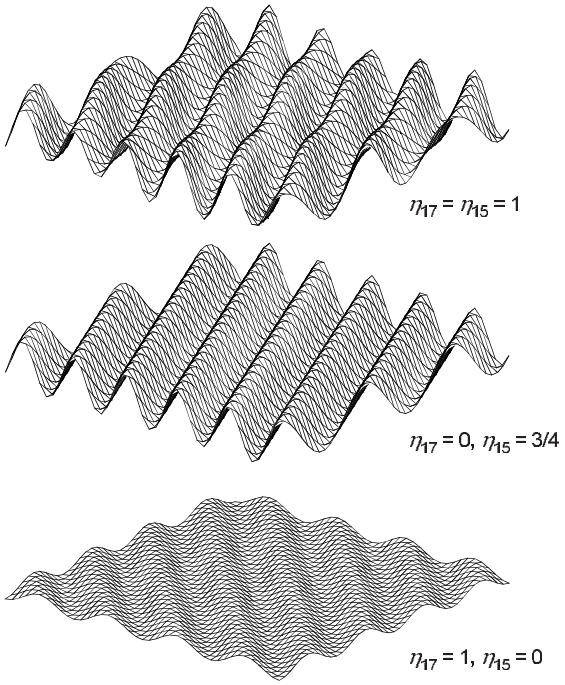

FIG. 13. Concentration waves in the nonmetal plane $(1-11)_{L'3}$ of the ordered trigonal (space group $P\bar{3}1m$) carbide ε-W_2C at different values of the long-range order parameters η_{17} and η_{15}.

the orthorhombic phase β'-W_2C with the ζ-Fe_2N structure is observed in W_2C samples only after annealing at $T < 1300$ K. Thus, annealing at 1370 K does not lead to the formation of the ordered orthorhombic phase and decomposition of the lower tungsten carbide to WC and W.

Samples of $WC_{0.35}$, $WC_{0.50}$, and $WC_{0.70}$ were synthesized by sintering of a W+C mixture in a vacuum at 1370 K. The sintering time was 30 h. Then, the sintered samples were ground, compacted again, and sintered at the same temperature of 1370 K for 20 h. XRD patterns of all the samples sintered for 30 h contain reflections of the lower tungsten carbide W_2C along with those of tungsten W and the higher carbide WC (Fig. 14). The concentration of W_2C is the maximum in the $WC_{0.50}$ sample since its composition corresponds to the stoichiometric lower carbide. As the sintering time increased to 50 h, the concentrations of W and W_2C decreased and increased, respectively. The observed formation of W_2C in the samples sintered from tungsten and carbon at 1370 K and the growth of the W_2C concentration in these samples with the increase of sintering time contradict the assumption[11,27,28] of the eutectoid decomposition of the lower carbide W_2C to W and WC at $T \leqslant 1530$ K. Tungsten is present in all the samples because they were synthesized at a low temperature and synthesis was not complete even after 50 h.

For comparison, samples of $WC_{0.35}$, $WC_{0.50}$, and $WC_{0.70}$ were synthesized from tungsten and carbon powder mixtures at 1870 K for 5 h. Synthesis was almost complete at this temperature and, therefore, just two phases were present in the samples (~43 wt % W and ~57 wt % W_2C in $WC_{0.35}$; ~9 wt % W and ~91 wt % W_2C in $WC_{0.50}$; ~86 wt % W_2C and ~14 wt % WC in $WC_{0.70}$).

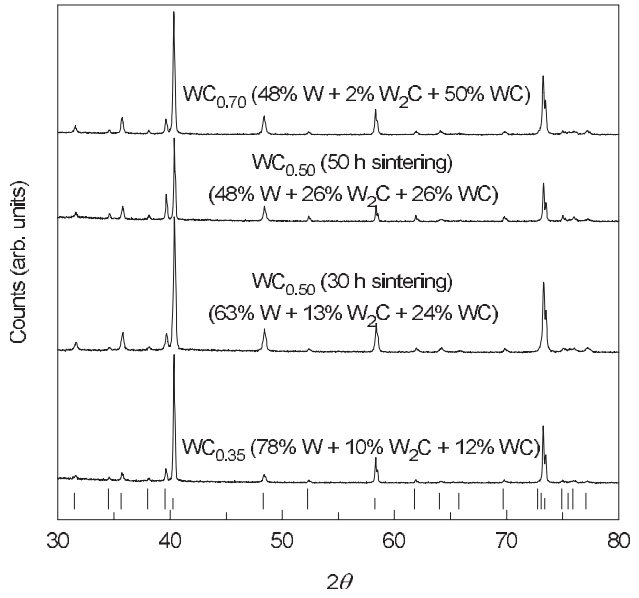

FIG. 14. XRD patterns of $WC_{0.35}$, $WC_{0.50}$, and $WC_{0.70}$ samples synthesized from a W+C mixture by sintering at 1370 K for 30 h and the $WC_{0.50}$ sample prepared by sintering at the same temperature for 50 h. The lower tungsten carbide W_2C is present in all the samples. The content of the W_2C phase is the maximum in the $WC_{0.50}$ sample, which is the closest to the stoichiometric composition of the lower carbide. The W_2C content grows as the sintering time increases to 50 h. The phase composition is given in wt %. Long, middle, and short ticks correspond to reflections of W_2C, WC, and W phases, respectively. Cu $K\alpha_{1,2}$ radiation.

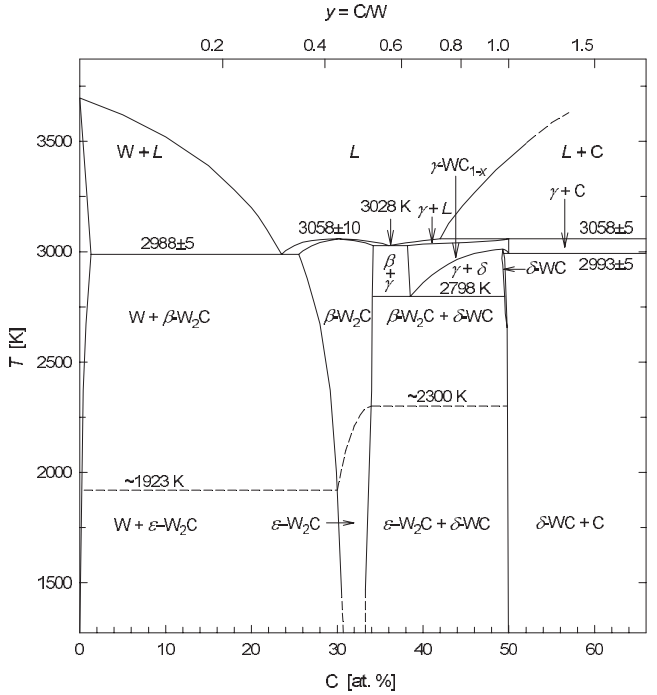

FIG. 15. Phase diagram of the W-C system. Ordered trigonal phases ε-W_2C experimentally detected in Refs. 8, 19, and 21–25 and in this study are thermodynamically stable in the temperature interval of ~2300–1300 K. Phase boundaries of the cubic tungsten carbide γ-$WC_{1-x} \equiv \gamma$-WC_y, are shown, as reported in Ref. 39. Singular points of the diagram are given in Table VI.

Thus, the experiment demonstrated that the lower tungsten carbide W_2C is thermodynamically stable from the melting point of ~3050–1370 K and does not decompose over this temperature interval. At temperatures of ~2300–1370 K, the only ordered phase of the lower tungsten carbide W_2C is the trigonal (space group $P\bar{3}1m$) phase ε-W_2C. Traces of the ordered orthorhombic (space group $Pbcn$) phase β'-W_2C were not detected even after long-time annealing at 1370 K. The transition from the ordered trigonal phase ε-W_2C to the ordered orthorhombic (space group $Pbcn$) phase β'-W_2C is probable to occur at a temperature below 1370 K. According to Refs. 15, 16, and 20, the orthorhombic (space group $Pbcn$) phase β'-W_2C with the ζ-Fe_2N structure indeed is observed in samples of the lower tungsten carbide at a temperature below 1300 K.

VII. REFINEMENT OF PHASE DIAGRAM OF W-C SYSTEM

Refinement of the phase diagram of the W-C system is related essentially to the existence range of the carbide W_2C and its ordered phases. It follows from the above x-ray and neutron diffraction analyses that the ordered trigonal (space group $P\bar{3}1m$) phase ε-W_2C exists in samples synthesized over a wide temperature interval of ~2300–1370 K. No traces of other ordered phases were detected. The concentration of the ordered phase ε-W_2C was much smaller (nearly seven times) than the concentration of the disordered phase β-W_2C in samples prepared by plasma chemical synthesis at a high temperature. The phase ε-W_2C appears in these samples quenched from 2300 to 2400 K because the reaction occurs in strongly nonequilibrium conditions. The obtained results are in agreement with the literature data,[8,20,22–26] according to which the only ordered trigonal phase ε-W_2C is detected in samples of the lower tungsten carbide prepared by different methods at temperatures of ~1900–2300 K. Thus, trigonal (space group $P\bar{3}1m$) phase ε-W_2C is formed at a temperature of ~1900–2300 K most likely by the mechanism of the second-order phase transition.

Long-time low-temperature (1370 K) annealing of samples containing the ordered phase ε-W_2C did not change their phase composition. It means that the ε-W_2C superstructure is stable at this temperature. When WC_y samples (y=0.35,0.50,0.70) were synthesized at 1870 K and at a lower temperature of 1370 K by sintering of W+C powder mixtures, all of them contained the lower tungsten carbide W_2C. The content of W_2C phase depends on the sample composition and is the maximum in the $WC_{0.50}$ sample. Direct synthesis of the carbide W_2C from tungsten and carbon at 1370 and 1870 K means that the lower carbide is in thermodynamic equilibrium at these temperatures. Taking into account the data on low-temperature annealing of W_2C, it can be stated that the lower tungsten carbide is thermodynamically stable at $\geqslant$1370 K and does not undergo solid-phase decomposition at ~1530 K, as supposed in Refs. 9–11, 27, and 28.

TABLE VI. Special points in the phase diagram of the W-C system (Fig. 15) at a temperature above 1300 K.

Reaction	Composition of phases involved in the reaction (at. % of C)			T (K)	Reaction type
$L \Leftrightarrow W$	0	0		3755±5	Melting
$L \Leftrightarrow \beta\text{-}W_2C$	~30.2	~30.2		3058±10	Congruent melting
$L+C \Leftrightarrow \gamma\text{-}WC_{1-x}$[a]	~42.0	100.0	50.0	3058±5	Peritectics
$L \Leftrightarrow W+\beta\text{-}W_2C$	~23.5	~1.2	~25.5	2988±5	Eutectics
$L \Leftrightarrow \beta\text{-}W_2C+\gamma\text{-}WC_{1-x}$[a]	~36.0	~34.2	~38.2	3028±5	Eutectics
$\gamma\text{-}WC_{1-x} \Leftrightarrow \delta\text{-}WC$[a]	~49.3	~49.3		3012±5	Polymorphic transformation
$\gamma\text{-}WC_{1-x} \Leftrightarrow \delta\text{-}WC+C$[a]	50.0	~49.8	100.0	2993±5	Eutectoid decomposition
$\gamma\text{-}WC_{1-x} \Leftrightarrow \beta\text{-}W_2C+\delta\text{-}WC$[a]	~38.5	~34.0	~49.5	2798±5	Eutectoid decomposition
$\beta\text{-}W_2C \Leftrightarrow \varepsilon\text{-}W_2C$	~30.0–34.0	~30.0–34.0		~1920–2300	Disorder-order transformation

[a] $\gamma\text{-}WC_{1-x} \equiv \gamma\text{-}WC_y$ $(y \equiv 1-x)$.

Taking into account experimental results related to the crystal structure and the temperature range of existence of the lower tungsten carbide and considering the literature data,[8,20,22–25] the positions of phase boundaries of the lower carbide W_2C are corrected, as shown in Fig. 15. Over the temperature interval of ~2300–1370 K, the phases β'-W_2C and β''-W_2C, not found experimentally, are replaced by the observed ordered phase ε-W_2C. This ordered phase does not undergo eutectoid decomposition at ~1530 K and is thermodynamically stable at least to a temperature of ~1370 K.

Kurlov and Gusev[40] analyzed a large number of literature data on the cubic tungsten carbide γ-WC_{1-x} and showed that this carbide exists as a one-phase compound over a narrow temperature interval of 3058–2798 K. The cubic tungsten carbide has a wide homogeneity interval from $WC_{0.61}$ to $WC_{1.00}$ at a temperature of ~3025 K, but a homogeneity interval quickly narrows with decreasing temperature and only the cubic carbide $WC_{0.62}$ exists at ~2800 K. At a temperature of ~2798 K, the cubic tungsten carbide γ-$WC_{0.62}$ undergoes eutectoid decomposition to the lower hexagonal W_2C and the higher hexagonal WC tungsten carbide. The phase boundaries of the cubic tungsten carbide γ-WC_{1-x} are shown in Fig. 15, as determined by Kurlov and Gusev.[40]

Singular points of the phase diagram of the W-C system (Fig. 15) are given in Table VI.

VIII. CONCLUSION

Experimental and theoretical studies of the structure of the lower tungsten carbide W_2C demonstrated that this carbide is thermodynamically stable from the melting point of ~3050 K to a temperature of 1370 K and does not decompose over this temperature interval. At temperatures of ~2300–1370 K, the only ordered phase of the lower tungsten carbide W_2C is the trigonal (space group $P\bar{3}1m$) phase ε-W_2C. Trigonal phase ε-W_2C is formed at a temperature of ~1900–2300 K most likely by the mechanism of the second-order phase transition. Thus, the experiments and theory show that the following sequence of phase transformations, disordered hexagonal (space group $P6_3/mmc$) phase β-$W_2C \rightarrow$ ordered trigonal (space group $P\bar{3}1m$) phase ε-W_2C, is realized. Probably, at temperatures below 1370 K, the trigonal phase ε-W_2C transforms to the orthorhombic phase β'-W_2C. This assumption does not contradict the theoretically possible sequence of phase transformations and is confirmed by results obtained in Refs. 15, 16, and 20. According to these results, the orthorhombic (space group $Pbcn$) phase β'-W_2C with the ζ-Fe_2N structure was observed in samples of the lower tungsten carbide annealed at temperatures below 1300 K. For the addition and specification of these literature data, *in situ* high-temperature neutron diffraction measurements are required.

ACKNOWLEDGMENTS

The authors are grateful to I. F. Berger for assistance in the neutron diffraction measurements. The authors are indebted to the Russian Foundation for Basic Research (Grants Nos. 06-03-32047 and 07-03-96066) for financial support.

[1] A. I. Gusev, A. A. Rempel, and A. J. Magerl, *Disorder and Order in Strongly Nonstoichiometric Compounds: Transition Metal Carbides, Nitrides and Oxides* (Springer, Berlin, 2001), p. 607.
[2] A. I. Gusev, *Nonstoichiometry, Disorder, Short-Range and Long-Range Order in Solids* (Nauka, Moscow, 2007), p. 856 (in Russian).
[3] H. Holleck, *Binäre und Ternäre Carbid-und Nitridsysteme der Übergangsmetalle* (Gebrüder Borntraeger, Berlin, 1984), p. 295.
[4] A. I. Gusev and A. A. Rempel, Phys. Status Solidi A **163**, 273 (1997).
[5] C. H. de Novion, B. Beuneu, T. Priem, N. Lorenzelli, and A. Finel, in *The Physics and Chemistry of Carbides, Nitrides and Borides*, edited by R. Freer (Kluwer, Dordrecht, 1990), pp. 329–355.
[6] *Materials Science of Carbides, Nitrides and Borides*, edited by Y. G. Gogotsi and R. A. Andrievski (Kluwer, Dordrecht, 1999), p. 360.
[7] A. S. Kurlov and A. I. Gusev, Russ. Chem. Rev. **75**, 617 (2006).
[8] K. Yvon, H. Nowotny, and F. Benesovsky, Monatsch. Chem. **99**, 726 (1968).
[9] E. Rudy and S. Windisch, J. Am. Ceram. Soc. **50**, 272 (1967).
[10] E. Rudy and J. R. Hoffman, Planseeber. Pulvermet. **15**, 174 (1967).
[11] E. Rudy, *Ternary Phase Equilibria in Transition Metal-Boron-Carbon-Silicon Systems. Compendium of Phase Diagram Data*, Final Tech. Report AFML Report No. TR-65-2 (Air Force Materials Laboratory, Ohio, 1969), p. 735.
[12] E. Parthe and V. Sadagopan, Acta Crystallogr. **16**, 202 (1963).
[13] P. Stecher, F. Benesovsky, and H. Nowotny, Planseeber. Pulvermet. **12**, 89 (1967).
[14] V. S. Telegus, E. I. Gladyshevskii, and P. I. Kripyakevich, Sov. Phys. Crystallogr. **12**, 813 (1967).
[15] V. S. Telegus, Yu. B. Kuz'ma, and M. A. Marco, Poroshk. Metall. (Kiev) **11**, 56 (1971).
[16] Yu. Z. Nozik, Yu. F. Lipin, and B. V. Kuvaldin, Izv. Akad. Nauk Latv. SSR. Ser. Fiz.-Tekh. **6**, 30 (1968).
[17] N. Morton, B. W. James, G. H. Wostenholm, and D. C. B. Hepburn, J. Opt. Commun. **29**, 423 (1972).
[18] V. Z. Kublii, T. Ya. Velikanova, O. A. Gnitetskii, and S. I. Makhovitskaya, Poroshk. Metall. (Kiev) **3/4**, 46 (2000).
[19] J. Dubois, T. Epicier, C. Esnouf, G. Fantozzi, and P. Convert, Acta Metall. **36**, 1891 (1988).
[20] T. Epicier, J. Dubois, C. Esnouf, G. Fantozzi, and P. Convert, Acta Metall. **36**, 1903 (1988).
[21] L. N. Butorina and Z. G. Pinsker, Sov. Phys. Crystallogr. **5**, 560 (1960).
[22] A. Harsta, S. Rundqvist, and J. O. Thomas, Acta Chem. Scand., Ser. A **A32**, 891 (1978).
[23] A. I. Gusev and A. S. Kurlov, JETP Lett. **85**, 34 (2007).
[24] B. Lönnberg, T. Lundström, and R. Tellgren, J. Less-Common Met. **120**, 239 (1986).
[25] T. Epicier, J. Dubois, C. Esnouf, and G. Fantozzi, Compt. Rend. Acad. Sci. Paris. Ser. II. **297**, 215 (1983).
[26] V. Z. Kublii, T. Ya. Velikanova, and B. V. Khaenko, Metal Physics Advanc. Technolog. **21**, 26 (1999).
[27] V. Z. Kublii and T. Ya. Velikanova, Powder Metall. Met. Ceram. **43**, 630 (2004).
[28] M. Gleiser and J. Chipman, Trans. Metall. Soc. AIME **224**, 1278 (1962).
[29] *Binary Alloy Phase Diagrams*, 2nd ed., edited by T. B. Massalski, P. R. Subramanian, H. Okamoto, and L. Kasprzak (ASM, Metals Park, OH, 1990), Vol. 1, pp. 895–896.
[30] R. V. Sara, J. Am. Ceram. Soc. **48**, 251 (1965).
[31] *Phase Equilibria Diagrams: Phase Diagrams for Ceramists*, edited by A. E. McHale (American Ceramic Society, Westerville, OH, 1994), Vol. X, pp. 272–273.
[32] A. C. Larson and R. B. von Dreele, *General Structure Analysis System (GSAS)* (LANSCE, Los Alamos, 2004), Los Alamos National Laboratory Report No. LAUR 86-748.
[33] B. E. Warren, B. L. Averbach, and B. W. Roberts, J. Appl. Phys. **22**, 1493 (1951).
[34] O. V. Kovalev, *Representations of the Crystallographic Space Groups: Irreducible Representations, Induced Representations and Corepresentation* (Gordon & Breach, Yverdon, 1993), pp. 390.
[35] A. G. Khachaturian, *Theory of Structural Transformations in Solids* (Wiley, New York, 1983), p. 574.
[36] A. I. Gusev and A. A. Rempel, *Nanocrystalline Materials* (Cambridge International Science, Cambridge, 2004), p. 149.
[37] A. I. Gusev, *Nanomaterials, Nanostructures, and Nanotechnologies* (Nauka, Moscow, 2005), p. 409 (in Russian).
[38] L. V. Zueva, V. N. Lipatnikov, and A. I. Gusev, Inorg. Mater. **36**, 695 (2000).
[39] V. N. Lipatnikov and A. I. Gusev, Inorg. Mater. **42**, 14 (2006).
[40] A. S. Kurlov and A. I. Gusev, Inorg. Mater. **42**, 121 (2006).